



## Study of the Stability and Chemical Reactivity of a Series of Tetrazole Pyrimidine Hybrids by the Density Functional Theory method (DFT)

AHISSAN DONATIEN EHOUMAN<sup>1\*</sup>, ADJOU MANI RODRIGUE KOUAKOU<sup>1</sup>, FATOGOMA DIARRASSOUBA<sup>1</sup>, HAKIM ABDEL AZIZ OUATTARA<sup>1</sup> and PAULIN MARIUS NIAMIEN<sup>2</sup>

<sup>1</sup>Laboratoire de Thermodynamique et Physico-Chimie du Milieu, UFR SFA, Université Nangui Abrogoua, 02 BP 801 Abidjan 02, Côte-d'Ivoire.

<sup>2</sup>Laboratoire de Constitution et Réaction de la Matière, UFR SSMT, Université Félix Houphouët-Boigny, Abidjan Cocody, 22 BP 582 Abidjan 22, Côte-d'Ivoire.

\*Corresponding author E-mail: ehoundona@gmail.com/dodolamour2000@yahoo.fr

<http://dx.doi.org/10.13005/ojc/370406>

(Received: March 24, 2021; Accepted: July 01, 2021)

### ABSTRACT

Our theoretical study of stability and reactivity was carried out on six (06) molecules of a series of pyrimidine tetrazole hybrids (PTH) substituted with H, F, Cl, Br, OCH<sub>3</sub> and CH<sub>3</sub> atoms and groups of atoms using the density function theory (DFT). Analysis of the thermodynamic formation quantities confirmed the formation and existence of the series of molecules studied. Quantum chemical calculations at the B3LYP/6-311G (d, p) level of theory determined molecular descriptors. Global reactivity descriptors were also determined and analyzed. Thus, the results showed that the compound PTH\_1 is the most stable, and PTH\_5 is the most reactive and nucleophilic. Similarly, the compound PTH\_4 is the most electrophilic. The analysis of the local descriptors and the boundary molecular orbitals allowed us to identify the preferred atoms for electrophilic and nucleophilic attacks.

**Keywords:** Global and local descriptors, DFT, Tetrazole Pyrimidine Hybrids (PTH), Chemical stability, Reactivity.

### INTRODUCTION

An infection, defined as an invasion of the organism by a foreign agent, namely a bacterium or a virus that can cause a pathological condition by injury to local cells. Among them, we have the invasive fungal infections (IFI), which can be caused by a variety of fungi such as yeasts, molds (*Aspergillus* spp) and dimorphic fungi (*Histoplasma capsulatum*) that are very common in some immunocompromised

patients<sup>1,2</sup>. We have more than 300 million people suffering from these diseases causing 1.35 million deaths each year in the world, which poses a real problem to the global health system<sup>2,3</sup>. In the face of this scourge, clinically available antifungal agents have been proposed for the treatment of these IFIs but they are quite limited<sup>4,5</sup> and most of them are not effective due to high resistance to toxicity and some adverse side effects<sup>6,7</sup>. Therefore, the development of new antifungal agents with low toxicity that will be



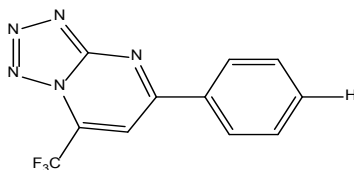
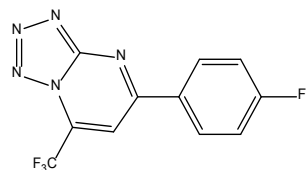
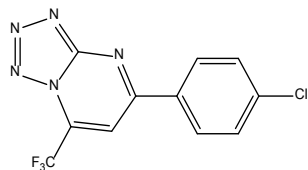
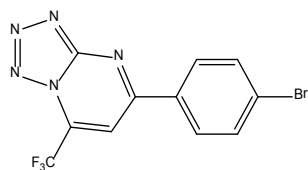
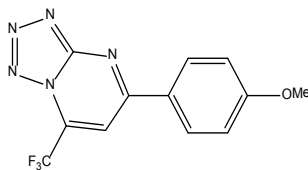
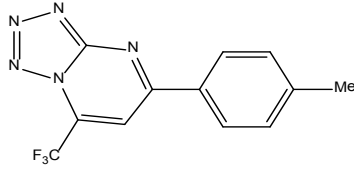
effective in the control of these fungi are in order. As a result, tetrazole hybrids have been synthesized and tested for their antifungal activities by Sheng-Qiang Wang *et al.*,<sup>8</sup> some of which have shown promising activity against drug-sensitive and drug-resistant fungi. Among these hybrids, we distinguish the pyrimidine associated with tetrazole which will give rise to a new series of molecules, namely Pyrimidine

tetrazole hybrids. This study will allow us to consider which of them are the most likely to act as antifungal.

## MATERIALS AND METHODS

This study was performed on six (06) molecules of the Pyrimidine tetrazole hybrid series presented in Table 1 below:

**Table 1: Structure of the studied Pyrimidine Tetrazole Hybrid derivatives**

Code	Brute formula	Structure and nomenclature
PTH_1	$C_{11}H_6F_3N_5$	 5-phenyl-7-(trifluoromethyl)tetrazolo[1,5-a]pyrimidine
PTH_2	$C_{11}H_5F_4N_5$	 5-(4-fluorophenyl)-7-(trifluoromethyl)tetrazolo[1,5-a]pyrimidine
PTH_3	$C_{11}H_5ClF_3N_5$	 5-(4-chlorophenyl)-7-(trifluoromethyl)tetrazolo[1,5-a]pyrimidine
PTH_4	$C_{11}H_5BrF_3N_5$	 5-(4-bromophenyl)-7-(trifluoromethyl)tetrazolo[1,5-a]pyrimidine
PTH_5	$C_{12}H_8F_3N_5O$	 5-(4-methoxyphenyl)-7-(trifluoromethyl)tetrazolo[1,5-a]pyrimidine
PTH_6	$C_{12}H_8F_3N_5$	 5-(p-tolyl)-7-(trifluoromethyl)tetrazolo[1,5-a]pyrimidine

### Software and theory level

The theoretical study of stability and chemical reactivity was carried out based on three theoretical approaches. The first approach relates to global descriptors deriving from frontier molecular orbitals and then the second approach is concerned with local indices of reactivity. The geometries of the molecules were optimized at the DFT calculation level with the B3LYP functional<sup>9-11</sup> in the 6-311 G (d, p) base using the Gaussian 09 software<sup>12</sup>. This Hybrid functional gives better energies and is in agreement with high level ab initio methods<sup>13-14</sup>. As for the split-valence and triple-dzeta base (6-311G (d, p)), it is sufficiently extensive and the consideration of polarization functions is important for the explanation of free doublets of heteroatoms. The geometries are kept constant for cationic and anionic systems. The global reactivity indices were obtained from the conceptual DFT model<sup>15-17</sup>.

### Standard thermodynamic quantities of formation

The thermodynamic quantities of the molecules were performed from optimization and calculation of frequencies at the B3LYP/6-311G (d, p) level. The quantities such as entropy, enthalpy and free enthalpy of formation were determined using the following formulas proposed by Otchersky *et al.*,<sup>11</sup>.

$$\Delta_f H^0(M, 0K) = \sum_{atoms} x \Delta_f H(X, 0K) - \sum D_0 \quad (1)$$

$$\begin{aligned} \Delta_f H^0(M, 298K) \\ = \Delta_f H^0(M, 0K) + (H_M^0(298K) - H_M^0(0K)) \\ - \sum_{atoms} x (H_X^0(298K) - H_X^0(0K)) \end{aligned} \quad (2)$$

Where:

$$\sum D_0 = \sum x \varepsilon_0 - \varepsilon_0(M) - \varepsilon_{ZPE} \quad (3)$$

$\sum D_0$  : Atomization energy;

$\varepsilon_0(M)$  : Total energy of the molecule;

$\varepsilon_{ZPE}$  : Zero-point energy of the molecule;

$H_X^0(298K) - H_X^0(0K)$  : Enthalpy corrections of atomic elements. These values are included in the Janaf table<sup>19</sup>.

$H_M^0(298K) - H_M^0(0K) = H_{corr} - \varepsilon_{ZPE}(M)$  : Molecule enthalpy correction.

$H_{corr}$  : Enthalpy of thermal correction

$$\Delta_f S^0(M, 298K) = S_M - \sum_{atoms} x \Delta S(298K) \quad (4)$$

x : Number of atoms in the Molecule

$$\Delta_f G^0(M, 298K) = \Delta_f H^0(M, 298K) - T \Delta_f S^0(M, 298K) \quad (5)$$

### Reactivity descriptors

#### Global descriptors

To predict chemical reactivity, some theoretical descriptors related to conceptual DFT have been determined. In particular, the energy of the Lowest Unoccupied molecular orbital (ELUMO), the energy of the Highest occupied molecular orbital (EHOMO), electronegativity ( $\chi$ ), softness global ( $\sigma$ ) and the global electrophilicity index ( $\omega$ ). These descriptors are all determined from the optimized molecules. It should be noted that the descriptors related to the frontier molecular orbitals have been calculated in a very simple way within the framework of the Koopmans approximation<sup>18</sup>. LUMO energy characterizes the sensitivity of the molecule to nucleophilic attack, and HOMO energy characterizes the susceptibility of a molecule to electrophilic attack. Electronegativity ( $\chi$ ) is the parameter that reflects the ability of a molecule not to let its electrons escape. The overall softness ( $\sigma$ ) expresses the resistance of a system to a change in its number of electrons. The overall electrophilicity index characterizes the electrophilicity of the molecule. These different parameters are calculated from equations (6).

$$\begin{aligned} I &= -E_{\text{HOMO}} \\ A &= -E_{\text{LUMO}} \\ \chi &= -\mu = -\frac{E_{\text{LUMO}} + E_{\text{HOMO}}}{2} \\ \eta &= \frac{E_{\text{LUMO}} - E_{\text{HOMO}}}{2} \quad \omega = \frac{\chi^2}{2\eta} \\ \sigma &= \frac{1}{\eta} \end{aligned} \quad (6)$$

#### Local Fukui indices

The local responsiveness study was also conducted by determining the local Fukui indices. Two indices were used.

The electrophilic Fukui function  $f^+$  which characterizes the electron density response to electron gain and gives information on the most electrophilic site toward nucleophilic attack and the function of nucleophilic Fukui  $f^-$  characterizing the electron density response to electron loss and provides information on the most nucleophilic site toward an electrophilic attack.

It has been shown<sup>19</sup>, for reactions controlled by frontier orbitals, that a high value of the Fukui index means high reactivity of the site. The condensed form of these two functions in the case of a molecule with  $N$  electrons has been proposed by Yang and Mortier<sup>20</sup>:

$$f^+ = q_k(N + 1) - q_k(N) \quad (7)$$

$$f^- = q_k(N) - q_k(N - 1) \quad (8)$$

## RESULTS AND DISCUSSION

### Study of standard thermodynamic formation parameters

The thermodynamic parameters, namely the enthalpy of formation  $\Delta_f H^\circ$ , the entropy of formation  $\Delta_f S^\circ$  and the free enthalpy of formation  $\Delta_f G^\circ$  were also determined. It should be noted that the enthalpy reflects the thermicity of a chemical reaction when entropy provides information on the level of disorder in the system. In addition, the free enthalpy reflects the possibility or not of a chemical reaction.

The values of the thermodynamic parameters are given in Table 2.

**Table 2: Thermodynamic quantities of PTH formation optimized at the theory level B3LYP / 6-311G (d, p)**

Molecule	$\Delta_f H^\circ_{298}$ (kcal/mol)	$\Delta_f S^\circ_{298}$ (cal/mol.K)	$\Delta_f G^\circ_{298}$ (kcal/mol)
PTH_1	-982.1206	-755.3723	-756.9064
PTH_2	-1050.5583	-761.2891	-823.5800
PTH_3	-982.1498	-760.0310	-755.5466
PTH_4	-971.4305	-759.4040	-745.0142
PTH_5	-1131.1434	-871.9923	-871.1589
PTH_6	-1039.4355	-837.8549	-789.6291

The results show that all the values of the standard thermodynamic quantities of molecule formation are negative. This means that during the formation of all the PTH compounds occurs spontaneously with a release of heat and a reduction in disorder. At this level, we note that the quantities determined at the level of theory B3LYP/6-311G (d, p) confirm the formation and existence of the series of Pyrimidine tetrazole hybrids explored.

### Global reactivity indices

The conceptual DFT descriptors determined have contributed in several ways to understanding the structure of molecules and their reactivity. The reactivity parameters examined in this series of compounds are: chemical potential ( $\mu$ ), hardness

( $\eta$ ), softness (S) and electrophilic index ( $\omega$ ). The calculated values of said parameters are reported in Table (3).

**Table 3: Summary of global reactivity descriptors at the B3LYP/ 6-311G theory level (d, p)**

Molecule	$\mu$ (eV)	$\eta$ (eV)	S (eV-1)	$\omega$ (eV)
PTH_1	5.2518	2.1107	0.4738	6.5338
PTH_2	5.2806	2.0671	0.4838	6.7449
PTH_3	5.3283	2.0304	0.4925	6.9913
PTH_4	5.2838	1.9905	0.5024	7.0127
PTH_5	4.8228	1.8757	0.5331	6.2002
PTH_6	5.0925	2.0401	0.4902	6.3560

The chemical potential values recorded for the Pyrimidine tetrazole hybrids in Table 3 indicate that PTH\_3 is the molecule most likely to retain its electrons due to its fairly high chemical potential value compared to others.

In terms of chemical hardness ( $\eta$ ) and overall softness (S), the hardness increases with the stability of the molecule while the softness increases with the reactivity of the molecule. Thus, the harder a molecule, the more stable and less reactive it is. This is the case with PTH\_1, which is the hardest molecule, and therefore the least reactive of all, because it has the highest hardness value ( $\eta$ ). The PTH\_5 molecule, on the other hand, is the softest of all molecules, hence the most reactive. Methoxy therefore contributes to increasing the reactivity of the molecule.

With regard to the electrophilic index ( $\omega$ ), a molecule is all the more electrophilic the higher the value of the overall electrophilic index, the molecule exhibiting the greater value of the electrophilic index is PTH\_4 while the compound PTH\_5 is the least electrophilic because it has the lowest value. Considering the other values in the table, we deduce that the halogens contribute to the increase in the electrophilic character of our molecules while the electron-donor groups decrease this character.

### Local descriptors

Since the dimerization of a biologically active molecule is likely to result in a biologically active molecule, we have therefore found it necessary to search for sites of nucleophilic and electrophilic attacks.

The Fukui indices, the frontier molecular orbitals HOMO and LUMO as well as the coefficients of the atomic orbitals in the frontier orbitals characterize the sites of electrophilic and nucleophilic attacks located for each molecule studied.

**Visualization of frontier molecular orbitals**

The analysis of the frontier molecular orbitals of PTH\_1 is given in Fig. 1 below:

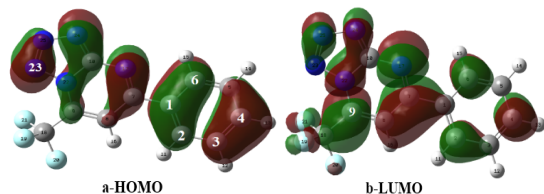


Fig. 1. PTH\_1 frontier molecular orbitals

**Observation of the frontier molecular orbitals of PTH\_1 shows that**

The atoms C<sub>1</sub>, C<sub>2</sub>, C<sub>3</sub>, C<sub>6</sub>, N<sub>23</sub> and C<sub>9</sub> being enclosed in the larger lobes of the HOMO are the atoms most susceptible to electrophilic attacks and those, contained in the larger lobes of the LUMO, to namely C<sub>9</sub> and C<sub>7</sub> are the sites of nucleophilic attacks.

The analysis of the frontier molecular orbitals of PTH\_2 is given in Fig. 2 below:

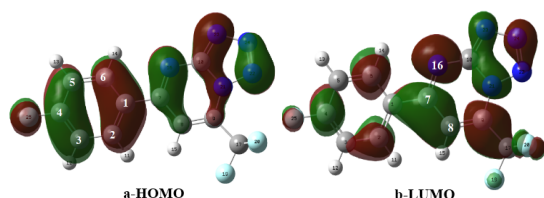


Fig. 2. Frontier molecular orbitals of PTH\_2

**Observation of the frontier molecular orbitals of PTH\_2 shows that**

The atoms C<sub>1</sub>, C<sub>2</sub>, C<sub>3</sub>, C<sub>4</sub>, C<sub>5</sub>, C<sub>6</sub> and N<sub>23</sub> being enclosed in the larger lobes of HOMO are the atoms most susceptible to electrophilic attacks and those contained in the larger lobes of LUMO, namely C<sub>8</sub>, C<sub>7</sub> and N<sub>16</sub> are the sites of nucleophilic attacks.

The analysis of the frontier molecular orbitals of PTH\_3 is given in Fig. 3 below:

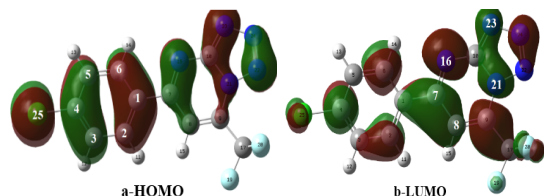


Fig. 3. Frontier molecular orbitals of PTH\_3

**Observation of the frontier molecular orbitals of PTH\_3 shows that**

The atoms C<sub>1</sub>, C<sub>2</sub>, C<sub>3</sub>, C<sub>4</sub>, C<sub>5</sub>, C<sub>6</sub> and Cl<sub>25</sub>

being enclosed in the larger lobes of HOMO are the atoms most susceptible to electrophilic attacks and those contained in the larger lobes of LUMO, namely C<sub>8</sub>, C<sub>7</sub>, N<sub>16</sub>, N<sub>21</sub> and N<sub>23</sub> are the sites of nucleophilic attacks.

The analysis of the frontier molecular orbitals of PTH\_4 is given in Fig. 4 below:

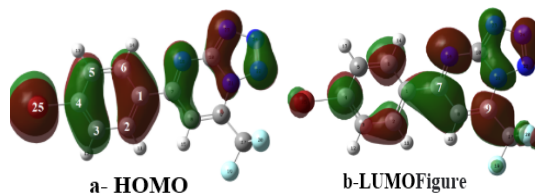


Fig. 4. Frontier molecular orbitals of PTH\_4

**Observation of the frontier orbital map of PTH\_4 shows that:**

The atoms C<sub>1</sub>, C<sub>2</sub>, C<sub>3</sub>, C<sub>4</sub>, C<sub>5</sub>, C<sub>6</sub> and Br<sub>25</sub> being enclosed in the larger lobes of HOMO are the atoms most susceptible to electrophilic attacks and those contained in the larger lobes of LUMO, namely C<sub>7</sub> and C<sub>9</sub> are the sites of nucleophilic attacks.

The analysis of the frontier molecular orbitals of PTH\_5 is given in Fig. 5 below:

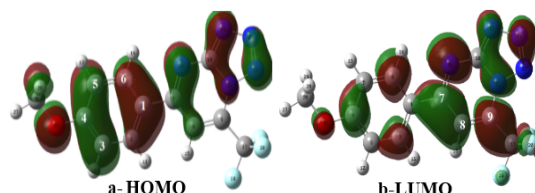


Fig. 5. Frontier molecular orbitals of PTH\_5

**Observation of the frontier orbital map of PTH\_5 shows that:**

The atoms C<sub>1</sub>, C<sub>3</sub>, C<sub>4</sub>, C<sub>5</sub> and C<sub>6</sub> being enclosed in the larger lobes of the HOMO are the atoms most likely to undergo electrophilic attacks and those, contained in the larger lobes of the LUMO, namely C<sub>7</sub>, C<sub>8</sub> and C<sub>9</sub> are the sites of nucleophilic attacks.

The analysis of the frontier molecular orbitals of PTH\_6 is given by the following Figure 6.

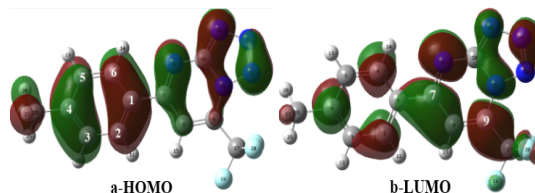


Fig. 6. Frontier molecular orbitals of PTH\_6

**Observation of the frontier orbital map of PTH\_6 shows that:**

The atoms C<sub>1</sub>, C<sub>2</sub>, C<sub>3</sub>, C<sub>4</sub>, C<sub>5</sub> and C<sub>6</sub> being enclosed in the larger lobes of the HOMO are the atoms most susceptible to electrophilic attacks and those, contained in the larger lobes of the LUMO, to namely C<sub>7</sub> and C<sub>9</sub> are the sites of nucleophilic attacks.

The visualization of the frontier molecular orbitals indicates for a given molecule, several sites of electrophilic and nucleophilic attacks. However, to be better situated on the most probable electrophilic and nucleophilic site, the calculation of the local Fukui indices was carried out.

**Calculation of Fukui indices**

The calculation of the Fukui indices of PTH\_1 allows us to obtain the values recorded in Table 4.

**Table 4: Values of local Fukui indices, calculated at the B3LYP/6-311G (d, p) level, according to NPA (Natural Population Analysis) for PTH\_1**

Atome	$f^+$	NPA	$f^-$
C <sub>8</sub>	0.0036		0.0044
C <sub>9</sub>	0.1503		0.0404
C <sub>10</sub>	-0.017		0.0038
N <sub>17</sub>	0.1413		0.0843
C <sub>18</sub>	0.0076		-0.002
F <sub>19</sub>	0.0264		0.0145
F <sub>20</sub>	0.0202		0.0129
F <sub>21</sub>	0.0265		0.0144
N <sub>22</sub>	0.0235		0.002
N <sub>23</sub>	0.0443		0.121

Analysis of the data in Table 4 indicates that the N<sub>23</sub> atom has the highest nucleophilic fukui index for the population analysis used when C<sub>9</sub> displays the highest electrophilic fukui index. Therefore, any electrophilic attack will preferentially be on the N<sub>23</sub> atom while a nucleophilic attack will be on the C<sub>9</sub> atom.

With regard to the TPH\_2 molecule, the calculation of its Fukui indices leads to the values shown in Table 5.

**Table 5: Values of local Fukui indices, calculated at the B3LYP/6-311G (d, p) level, according to NPA (Natural Population Analysis) for TPH\_2**

Atome	$f^+$	NPA	$f^-$
C <sub>1</sub>	-0.0300		0.1199
C <sub>2</sub>	0.0064		0.0222
C <sub>3</sub>	-0.004		0.0587
C <sub>4</sub>	0.0153		0.1027
C <sub>5</sub>	-0.006		0.0294
C <sub>6</sub>	0.0184		0.0365
C <sub>7</sub>	0.1001		-0.0010
C <sub>8</sub>	-0.015		0.0041
C <sub>9</sub>	0.0982		0.0385
C <sub>10</sub>	-0.1740		0.0033
N <sub>16</sub>	0.2956		0.0832

Analysis of the data in Table 5 indicates that atom C<sub>1</sub> has the highest nucleophilic fukui index for the population analysis used when N<sub>16</sub> displays the highest electrophilic fukui index. Therefore, any electrophilic attack will preferentially be on the N<sub>16</sub> atom when a nucleophilic attack will be on the C<sub>1</sub> atom.

The calculation of the Fukui indices of TPH\_3 leads to the values shown in Table 6.

**Table 6: Values of local Fukui indices, calculated at the B3LYP/6-311G (d, p) level, according to NPA (Natural Population Analysis) for TPH\_3**

Atome	$f^+$	NPA	$f^-$
C <sub>10</sub>	-0.0170		0.0030
N <sub>16</sub>	0.1373		0.0748
C <sub>17</sub>	0.0066		-0.0020
F <sub>17</sub>	0.0253		0.0133
F <sub>18</sub>	0.0193		0.0112
F <sub>19</sub>	0.0254		0.0132
F <sub>20</sub>	0.0242		0.0041
N <sub>21</sub>	0.0439		0.1041
N <sub>22</sub>	0.0691		0.1022
N <sub>23</sub>	0.0696		0.0362
Cl <sub>25</sub>	0.0762		0.1792

Analysis of the values in Table 6 shows that the N<sub>16</sub> atom has the highest electrophilic fukui index while the Cl<sub>25</sub> atom has the highest nucleophilic fukui index. All nucleophilic attacks will preferentially go to the N<sub>16</sub> atom and all electrophilic attacks will go to the Cl<sub>25</sub> atom.

The calculation of the Fukui indices of TPH\_4 leads to the values shown in Table 7.

**Table 7: Values of local Fukui indices, calculated at the B3LYP/6-311G (d, p) level, according to NPA (Natural Population Analysis) for TPH\_4**

Atome	$f^+$	NPA	$f^-$
C <sub>9</sub>	0.1428		0.0339
C <sub>10</sub>	-0.0170		0.0023
N <sub>16</sub>	0.1365		0.0699
C <sub>17</sub>	0.0065		-0.0011
F <sub>18</sub>	0.0250		0.0127
F <sub>19</sub>	0.0192		0.0104
F <sub>20</sub>	0.0252		0.0126
N <sub>21</sub>	0.0243		0.0048
N <sub>22</sub>	0.0436		0.0965
N <sub>23</sub>	0.0687		0.0943
N <sub>24</sub>	0.0691		0.0352
Br <sub>25</sub>	0.0889		0.2414

Analysis of the data in Table 7 indicates that the Br<sub>25</sub> atom has the highest nucleophilic fukui index for the population analysis used when C<sub>9</sub> displays the highest electrophilic Fukui index. Therefore, any electrophilic attack will be on the Br<sub>25</sub> atom while a nucleophilic attack will be on the C<sub>9</sub> atom.

The calculation of the Fukui indices of TPH\_5 leads to the values shown in Table 8.

**Table 8: Values of local Fukui indices, calculated at the B3LYP/6-311G (d, p) level, according to NPA (Natural Population Analysis) for TPH\_5**

Atome	NPA	
	$f^-$	$f^+$
C <sub>1</sub>	-0.0380	0.1441
C <sub>2</sub>	0.0265	0.0003
C <sub>3</sub>	0.0202	0.0816
C <sub>4</sub>	0.0728	0.0682
C <sub>5</sub>	0.0091	0.0483
C <sub>6</sub>	0.0656	0.0251
C <sub>7</sub>	0.1223	-0.0240
C <sub>8</sub>	0.0084	0.0028
C <sub>9</sub>	0.1516	0.0325

Analysis of the values in this Table 8 indicates that atom C<sub>1</sub> has the highest nucleophilic fukui index for the population analysis used when C<sub>9</sub> displays the highest electrophilic fukui index. Therefore, any electrophilic attack will be on the C<sub>1</sub> atom while a nucleophilic attack will be on the C<sub>9</sub> atom.

Calculation of the fukui index of TPH\_6 leads to the values shown in Table 9.

**Table 9: Values of local Fukui indices, calculated at the B3LYP/6-311G (d, p) level, according to NPA (Natural Population Analysis) for HTP 6**

Atome	NPA	
	$f^-$	$f^+$
C <sub>1</sub>	-0.0330	0.1296
C <sub>2</sub>	0.0362	0.0213
C <sub>3</sub>	0.0154	0.0506
C <sub>4</sub>	0.0836	0.1417
C <sub>5</sub>	0.0097	0.0193
C <sub>6</sub>	0.0538	0.0358
C <sub>7</sub>	0.1248	-0.0090
C <sub>8</sub>	0.0040	0.0033
C <sub>9</sub>	0.1489	0.0357

Analysis of the data in Table 9 indicates that the highest nucleophilic fukui index value is obtained with the C<sub>4</sub> atom from which this atom is found to be the preferential center of all electrophilic attacks while the highest electrophilic fukui index is obtained with the C<sub>9</sub> atom. However, the latter will be the most likely site for nucleophilic attacks.

## CONCLUSION

At the end of our work, we retain that with

the level B3LYP/6-311G (d, p), we proceeded to the characterization of the sites of reactivity of the six (06) molecules of HTP. The values of the local Fukui indices indicated that the sites of reactivity vary depending on the substituent. Molecules with a halogen substituent have revealed that their nucleophilic attack sites are these halogens in question except fluorine whose nucleophilic site is on the C<sub>1</sub> atom. Regarding electrophilic sites, the C<sub>9</sub> atom is most likely for the molecules of HTP 1, HTP 4, HTP 5 and HTP 6.

The exploitation of the results obtained with the calculation of the global descriptors indicated to us that the HTP 1 molecule is the most stable of all, while the HTP 5 molecule is the most reactive with methoxy as a substituent. The substitution of halogens on the core of the HTP, indicates to us that the stability of our molecules increases with the halogens. Therefore, the more electronegative the halogen, the more stable the HTP molecules. The HTP 1 molecule has the greatest stability with hydrogen (H) as a substituent.

The calculation of the thermodynamic parameters allowed us to know that the formation of our hybrid tetrazole pyrimidine (HTP) molecules occurred spontaneously with the release of heat and reduction of disorder.

In perspective, we can consider to see what influence of temperature and pressure on the stability and reactivity of our series of molecules.

## ACKNOWLEDGEMENT

We are grateful to Professor ZIAO Nahossé, Director of the Laboratory of Thermodynamics and Physical Chemistry of the Environment, to Dr. BAMBA Kafoumba of the University NANGUI ABROGOUA (Ivory Coast), to Professor NIAMIEN Paulin Marius of the Laboratory of Constitution and Reaction of Matter of the University Félix Houphouët Boigny (Ivory Coast) for their support and motivation.

## REFERENCES

1. Brown, G. D.; Denning, D. W.; Gow, N. A.; Levitz, S. M.; Netea, M. G., & White, T. C. Hidden killers: human fungal infections. *Sci Transl Med.*, **2012**, *4*, 165-13.
2. Nam, S. I.; Aghebati-Maleki A., Morovati, H.; Aghebati-Maleki, L. *Biomed. Pharmacother.*, **2019**, *110*, 857-868.
3. Revie, N. M.; Iyer, K. R. ; Robbins, N.; Cowen, L. E. *Curr. Opin. Microbiol.*, **2018**, *45*, 70-76.

4. Joules, J.A.; MILLS. Blackwell Publishing House., **2000**, 507-511.
5. Butler R. N.; Katritzky, C.W. Rees, Eds., Pergamon Press: Oxford., **1984**, 5, 791.
6. Frederic, R B. *Chem. Rev.*, **1947**, 41, 1-61.
7. Ostrovskii, V. A.; Koren, A. O. *Heterocycles.*, **2000**, 53, 1421.
8. Amigoni, S. ; Fensterbank H.; Gaucher H. Ed Belin., **2004**.
9. Lee, C.; Yang, W.; Parr, R. *Physical Review Journals.*, **1988**, 37, 785.
10. Axel, B. D. *Journal of Chemical Physics.*, **1993**, 98, 5648.
11. Bédé, A. L.; Assoma, A. B.; Yapo, K. D.; Koné, M. G.-R.; Koné, S.; Koné, M.; N'Guessan, B.; Bamba, E.-H. S. *Computational Chemistry.*, **2018**, 6, 57-70.
12. Frisch, M. J.; Trucks, G. W.; Schlegel, H. B.; Scuseria, G. E.; Gaussian, Inc Gaussian 09, Revision A.02, Wallingford CT., **2009**.
13. Kapp, J.; Remko, M.; Schleyer, P. v. R. *Journal of the American Chemical Society.*, **1996**, 118, 5745-5757.
14. Johnson, B. G.; Gill, P. M.; Pople, J. A. *The Journal of Chemical Physics.*, **1993**, 98, 5612-5626.
15. Parr, R. G.; Yang, W. *Annual Review Physical Chemistry.*, **1995**, 46, 701-728.
16. Coulibaly, W. K.; N'dri, J.; Koné M. G.-R., Dago, C. D.; Ambeu, C. N.; Bazureau, J.-P.; Ziao N. *Computational Molecular Bioscience.*, **2019**, 9, 49-62.
17. Bohoussou, K. V.; Bénéié, A.; Koné G.-R. M.; Diki, N. Y. S.; Kouassi, K. A. R.; Ziao, N.; *Modern Chemistry.*, **2019**, 7, 38-44.
18. Koopmans, T.; *Physica.*, **1934**, 104-113.
19. Chattaraj, P. K.; Nath, S.; Sannigrahi, A. B.; *J. Phys. Chem.*, **1994**, 98, 9143.
20. Yang, W.; Mortier, W. J.; *J. Am. Chem. Soc.*, **1986**, 108, 5708.